# SUBPIXEL EDGE DETECTION WITH QUALITY INDICATOR AIDED TO PRESERVING THE DEPTH DISCONTINUITIES

Ting-Fang Chio[1] and Jen-Jer Jaw[1]
[1]National Taiwan University, No. 1, Sec. 4, Roosevelt Rd., Taipei 10617, Taiwan (R.O.C.),
Email:{ r05521116, jejaw}@ntu.edu.tw

**KEY WORDS:** Edge Detection, Subpixel, Depth Discontinuities

**ABSTRACT:** The integrity of geometric edge is vital to the high-quality 3-D scene representation. Thus, under the task of automated as well as successful 3-D scene or object reconstruction by photogrammetric approaches, edge detection and matching become an indispensable essential. Various edge detection techniques can only provide the locations of edge up to one pixel level, which may still incur significant intersection error when dealing with acute depth discontinuities. It was aimed in this study to obtain the subpixel accuracy of edge position to support dense image matching by image moment through appropriate function and weighting. In addition, an indicator giving the reliability of detected edges was also proposed. It was demonstrated that the proposed work scheme can support subpixel edge location on one hand and identify those weak edges to be denied or cautiously employed for the follow-up tasks, on the other hand.

## 1. INTRODUCTION

Dealing with depth discontinuities in dense stereo matching have been a challenging task. To tackle this problem, it needs to constraint supporting tuning penalty parameters and suitably handle depth discontinuity areas to ease the sensitiveness of SGM cost aggregation. To this end, edge detection and matching can be applied to provide plausible depth discontinuities. The common edge detection operators only provide the locations of edge up to one pixel level, which, however, is an insufficient accuracy if high geometric quality of positioning in such regions is attempted. This research aims to advance the edge detection up to subpixel accuracy, by solving the moment equation in the region of initial detected edges using Edge Drawing. When computing image moment, a weighting scheme is utilized to ease the image noise. In addition, the indicator to quantify the reliability of detected edges is proposed, so one can value these edges and use them for supporting depth discontinuities in dense stereo matching with more caution and thus improving the overall depth estimation.

## 2. RELATED WORK

In dense stereo matching, problems arising from image noise, textureless region, depth discontinuities and occlusions are quite common (Wei and Ngan, 2005; Chang and Ho, 2015; Chen et al., 2016). This research focuses on the problem of depth discontinuities. The methods of conquering depth discontinuities usually allocate different matching cost weighting for distinguishing foreground and background that causes depth discontinuities, so the matching cost or the penalty parameters of depth discontinuities can be eased (Wei and Ngan, 2005; Çiğla and Alatan, 2011; Sun et al.,2014; Chang and Ho, 2015; Chuang et al., 2016; Lee, 2016). Therefore, edge detection is a necessary stage in giving clues of depth continuities. But even edge detection is the most common task in computer vision, it is hard, if not possible, to find an existing algorithm to satisfy both subpixel accuracy and keeping integrity. (Maini and Aggarwal, 2009; Gupta et al., 2013; Gu et al., 2015). The moment-based, the least-square-error-based and the interpolation-based edge detection methods are potential to reach subpixel accuracy (Agustín et al., 2013). The moment-based approach uses the third-order image moment function to solve unknown edge position up to subpixel accuracy. On the other hand, the disadvantages of this approach is being sensitive to image noise, so small features may not be detected (Tabatabai et al., 1984; Lyvers et al., 1989; Qu et al., 2005; Hagara and Kulla, 2011). The least-square-error-based approach samples the gray level of image edges to be observations. It uses least squares method to correct observation and solve unknown edge position based on the ideal image edge model. This approach is more immune to image noise but the computing cost is huge (Agustín et al., 2013). The basic algorithm of interpolation-based approach is to transform the resolution of original images to higher resolution by using the resample methods, such as bilinear, bicubic, essentially non oscillatory (ENO) etc., to interpolate the grey level of higher resolution image (Hwang and Lee, 2004; Hermosilla et al., 2008; Agustín et al., 2013).

## 3. RESEARCH METHOD

Since the computing cost of least-square-error-based approach for edge detection is huge, and this study pursuits subpixel accuracy only in the direction of depth discontinuities. It turns out that the one-dimensional moment method is adopted to detect image edges within subpixel locations. Edge Drawing (Topal and Akinlar, 2012), which has better and stable result conquering image noise, is employed to have initial image edges with one pixel accuracy. Then based on these initial edges, the gray values and gradients of edge's region are sampled to compute the one-dimensional moment to solve subpixel edge location. Besides, an indicator giving the reliability of detected edge is proposed to effectively support edge constraints. To evaluate the accuracy of the detected edges to be within subpixel accuracy, the concept of down sampling is utilized. The disparity images provided by Scharstein *et al.* (2017) are tested by the proposed method and the promising results are concluded.

### 3.1 Edge Drawing

Gaussian smoothing is used as the first step in Edge Drawing to reduce image noise. The gradient operator follows to compute image gradient, including magnitude and direction. Then local maximum gradient is checked if it is bigger than the threshold. If yes, the pixel is marked as an "Anchor". And then starting from Anchors, nearby maximum gradient pixels with the same gradient direction are connected, and the procedure stops when meeting the end of the direction or repeating pixel that previously uses. The connecting step is called Smart Routing, shown as Figure 1. It evidently shows that the advantages of Edge Drawing are to offer precise and stable edge pixels and the segmented edges by Smart Routing.


Figure 1. The connection of Smart Routing. (Topal and Akinlar, 2012)

### 3.2 One-dimensional moment-based subpixel edge detection

The method proposed by Tabatabai *et al.* (1984) is shown in below. The computation of the third-order image moment is shown in Equation (1):

$$\bar{m}_i = \frac{1}{n}\sum_{j=1}^{n} x_j^i \text{，} i = 1,2,3 \tag{1}$$

In order to solve the edge position, one needs to solve three unknown variables, edge gray value $h_1, h_2$ and probability of edge gray value $p_1$, shown as Equations (2), (3-1) to (3-3).

$$\sum_{j=1}^{2} p_j h_j^i = \bar{m}_i \text{，} i = 1,2,3$$

$$where \quad \sum_{j=1}^{2} p_j = 1 \tag{2}$$

$$h_1 = \bar{m}_1 - \bar{\sigma}\sqrt{\frac{p_2}{p_1}} \tag{3-1}$$

$$h_2 = \bar{m}_1 + \bar{\sigma}\sqrt{\frac{p_1}{p_2}} \tag{3-2}$$

$$p_1 = 1 - \frac{1}{2}\left[1 + \bar{s}\sqrt{\frac{1}{4+\bar{s}^2}}\right] \tag{3-3}$$

*where*

$$\bar{\sigma}^2 = \bar{m}_2 - \bar{m}_1{}^2, \qquad \bar{s} \triangleq \frac{\bar{m}_3 + 2\bar{m}_1{}^3 - 3\bar{m}_1\bar{m}_2}{\bar{\sigma}^3}$$

Upon the solution, the probability of edge gray value $p_1$ and the number of sample $k$ determine the last position of edge gray value $h_1$, which is the targeted edge position.

## WEIGHTING OF OBSERVATION

To better estimate moment in taking the quality of the gradient observations into consideration, the Equation (4) is formulated by simply assigning weights in Equation (2).

$$\bar{m}_i = \frac{1}{\sum_{j=1}^{n} w_j} \sum_{j=1}^{n} x_j^i w_j \quad , i = 1,2,3 \tag{4}$$

The weight $w_j$ can be obtained by fitting an ideal gray level and gradient curve (Figure 2) to quantify the significance and stability of observations.

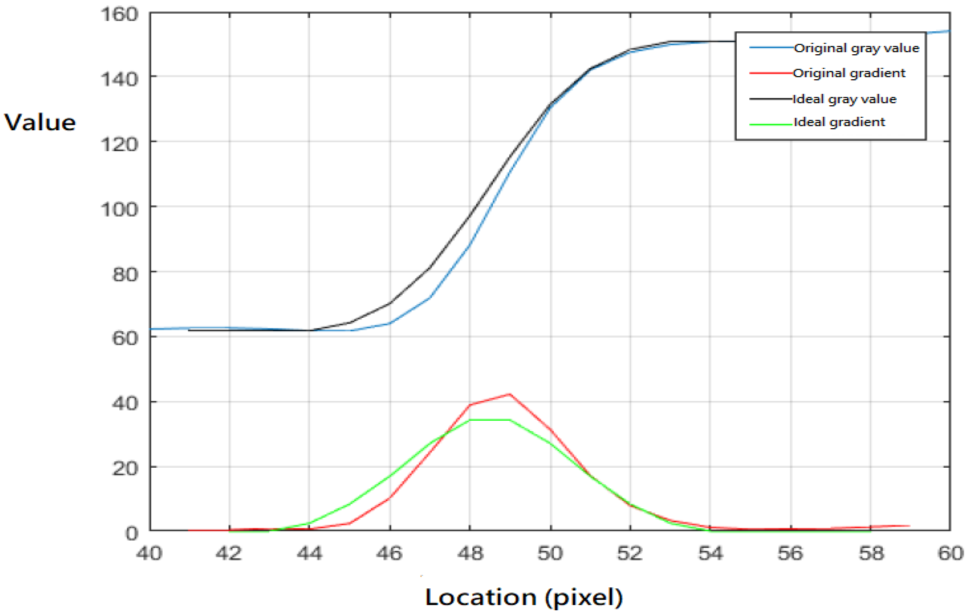


Figure 2. The ideal gray level and gradient curve

The ideal gradient value is employed to quantify the significance of observations, and the difference between the ideal gradient and the observed gradient is considered as the responses resulting from image noise and it reveals the stability of gradient observations. Equation (5) shows the weighting function:

$$w_j = \left(\frac{(\sum_{j=1}^{n} d_j) - d_j}{\sum_{j=1}^{n}((\sum_{j=1}^{n} d_j) - d_j)} + \frac{G_j}{\sum_{j=1}^{n} G_j}\right) / \sum_{j=1}^{n}(w_j) \tag{5}$$

*where*

$G_i$ = The ideal gradient

$d_i$ = The difference between the ideal gradient and the observed gradient

n = The sample number

## FITTING THE IDEAL GRAY VALUE CURVE

Assuming that the image blur edge produced by the Gaussian filter, this research samples the edge two side of gradient direction, which has first near zero gradient, to be upper bound and lower bound gray value. With Upper bound and lower bound gray value, edge curve without blur can be generated. And then, try different parameters of Gaussian filter on it, and select the parameter that has the smallest difference between the ideal and the observed gray value. According to the parameters of Gaussian filter, the ideal gray value curve and gradient curve can be computed. The procedure is shown in Figure 3.

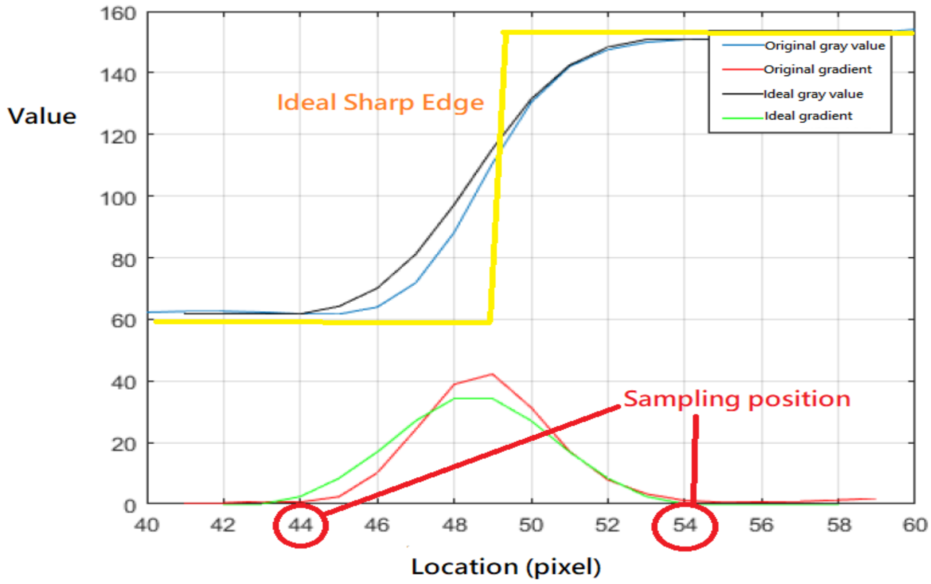


Figure 3. The illustration of fitting ideal gray level and gradient curve

### 3.3 PRIORI QUALITY INDICATOR OF DETECTED EDGES

To quantify the priori quality of detected edge, this research modifies the signal-to-noise ratio (S/N). The research uses the ratio of gradient and gradient standard deviation to be the indicator, which refers to the ratio of signal and noise. Equation (6) shows the indicator function:

$$\text{Priori quality of detected edge} = 10 \times \log\left(\frac{G_i}{\sigma}\right) \tag{6}$$

*where*

$G_i =$ The gradient of detected pixel , $\sigma =$ The gradient standard deviation of segmentated edge

This research also normalizes the indicator value to [0~1], because it is more convenient to observe every image phenomenon in the same scale. Equation (7) is the normalized function:

$$\text{The normalized indicator} = (\text{Original Value} - \min)/(\max - \min) \tag{7}$$

*where*

max = The maximum indicator value, min = The minimum indicator value

### 3.4 QUALITY EVALUATION

#### THE REAL DEPTH DISCONTINUITIES POSITION

The research uses 2 X 2 moving kernel (Figure 4) on real disparity image to detect depth discontinuities. If there are drastic disparity change between the central and the neighbour, the central will be the depth discontinuities or so called the geometric edge.

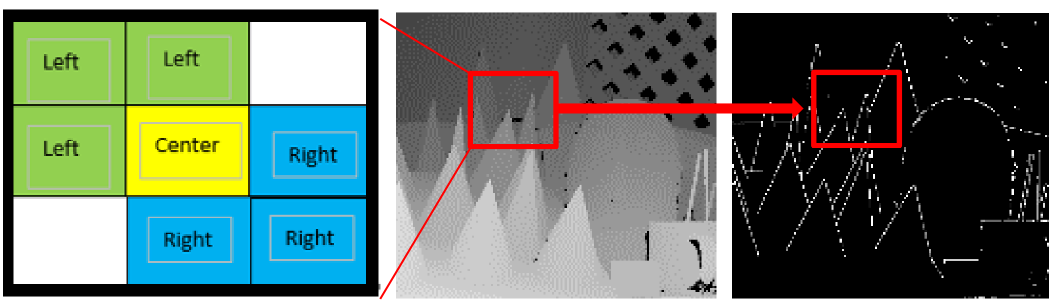


Figure 4. The moving kernel that detects depth discontinue pixel on the real disparity image.

## THE EVALUATION OF SUBPIXEL EDGE DETECTION

Like Figure 5, this research uses the concept of down sampling to evaluate the subpixel quality. In down sampling, this research uses the 10X10 average kernel to convolution with the high-resolution image, so the low-resolution width is 0.1 times the high-resolution width. According to that, this research can evaluate the minimum digit which is up to 0.1 pixel. In quality evaluation, this research first detects subpixel edges in the low-resolution image, then checks the integer position in low-resolution image. If the integer position is correct, check the subpixel position in the high-resolution region, which corresponds to the low-resolution. The searching method in the high-resolution region is shown in Figure 6. The method checks the edge position in gradient direction.

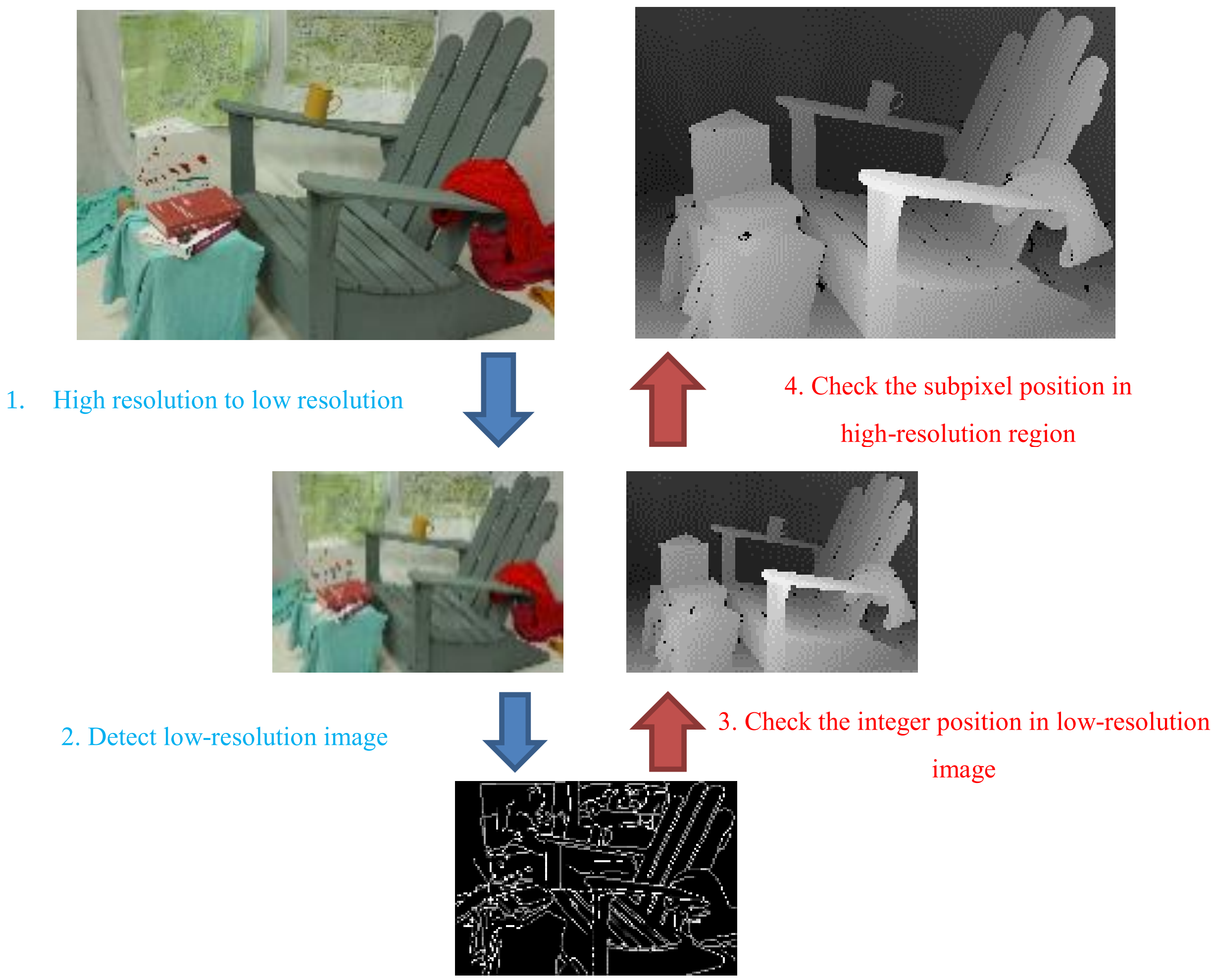


Figure 5. The procedure of evaluating subpixel quality.

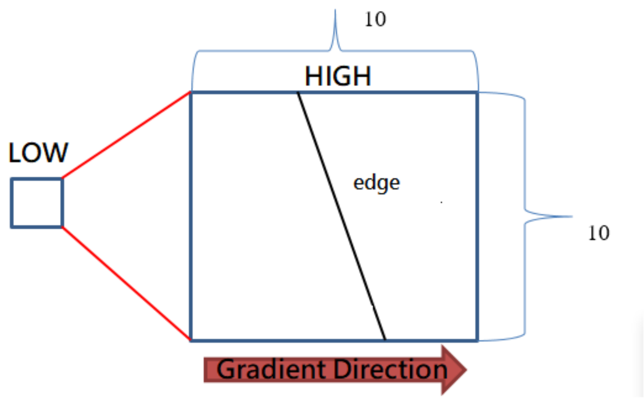


Figure 6. The searching illustration.

## 4. EXPERIMENTAL RESULTS

This research used 10 experimental stereo images with real subpixel disparity by Scharstein *et al.* (2017). The experimental stereo images are like Table 1, and the experimental parameters are like Table 2. In Table 2, the down sampling reduces the image width 10 times, so the minimum evaluated digit is up to 0.1 pixel.

Table 1. The experimental images

| Name | Size | Thumbnail | Name | Size | Thumbnail |
|---|---|---|---|---|---|
| Backpack | 2948X1988 |  | Sticks | 2856X2004 | 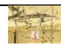 |
| Bicycle1 | 3052X1968 |  | Storage | 2792X1988 |  |
| Couch | 2296X1992 |  | Sword1 | 2928X2004 |  |
| Flowers | 2888X1984 |  | Sword2 | 2884X1956 |  |
| Mask | 2784X1992 |  | Umbrella | 2960X2008 |  |

Table 2. The experimental parameters

| | |
|---|---|
| Gaussian Smooth kernel size | 7 |
| Gaussian Smooth sigma | 1 |
| Gradient threshold | 30 |
| Anchor threshold | 5 |
| Number of Sampling in Subpixel detection | 6 |
| Down Sampling | 1/10 of original dimension |

The detected subpixel edge is shown in Figure 7. The red pixel means the subpixel position. One can see that those positions indeed depict the image edges in subpixel sense.

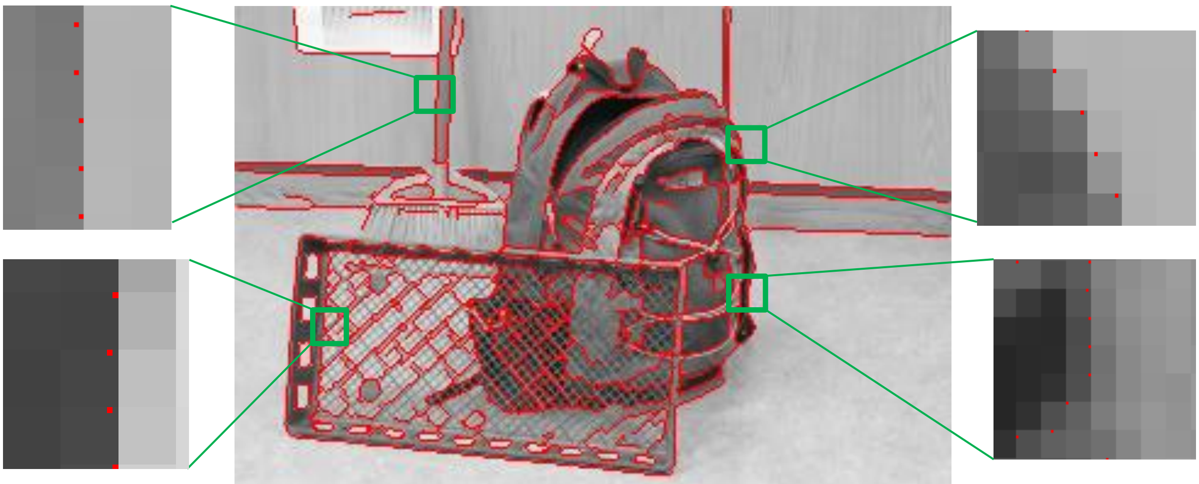

Figure 7. The subpixel edges of Backpack.

The distribution of indicator value in different kinds of detected edge's deviation is shown in Figure 8. Deviations are classified into three levels. The first level is that the deviation is smaller than 0.1 pixels, which means the correct detected edge in this quality evaluation. The second level of deviations range from 0.1 to 1 pixel, which is still in subpixel accuracy. The third level of deviations exceed 1 pixel. The indicator value in x-axis is normalized to [0, 1]. The percentage in y-axis means the indicator ratio in all detected edges.

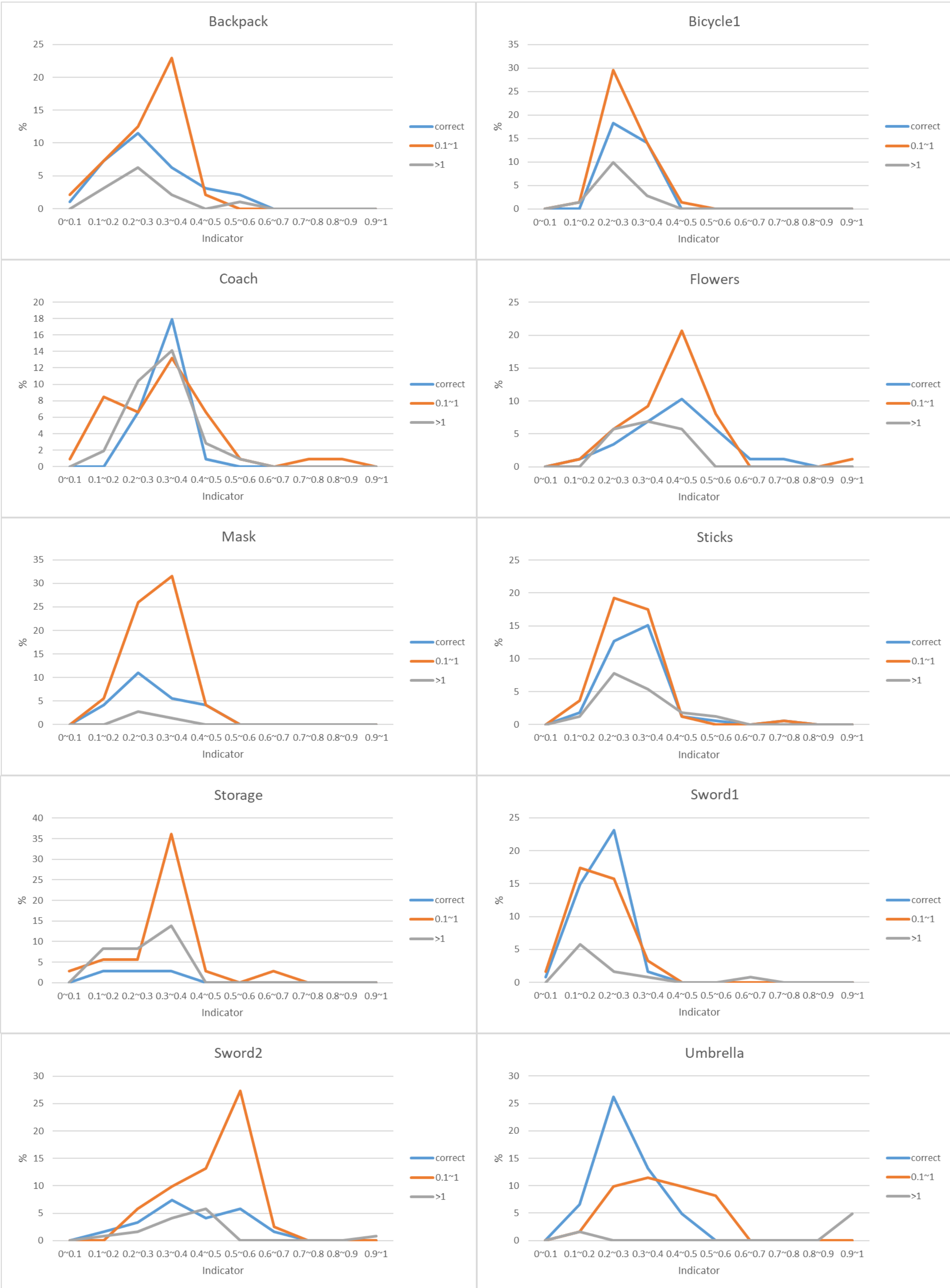


Figure 8. The distribution of indicator value in 3-kinds deviation level.

In Figure 8, the ratio of subpixel accuracy is higher than that of one pixel accuracy. The ratio represents that the approach can detect edges with subpixel accuracy properly. When the indicator grows, the indicator of subpixel accuracy grows more than one pixel accuracy, and the bigger indicator has more ratio of subpixel accuracy. It means that the indicator value can represent some information about edge quality. If the indicator is small, the detected edge deviation has more possibility out of one pixel. Otherwise, if the indicator is bigger, the detected edge deviation has more possibility in subpixel accuracy. So the bigger indicator represents the more reliable detected result, vice versa. The indicator values on the detected edges is shown in Figure 9. We can see that the higher value have more precise position. The lower value position mostly locates on the less featured region caused by the image noise or the image blur. The highest value position with red color almost locates at the image corner, which has the bigger gradient values.

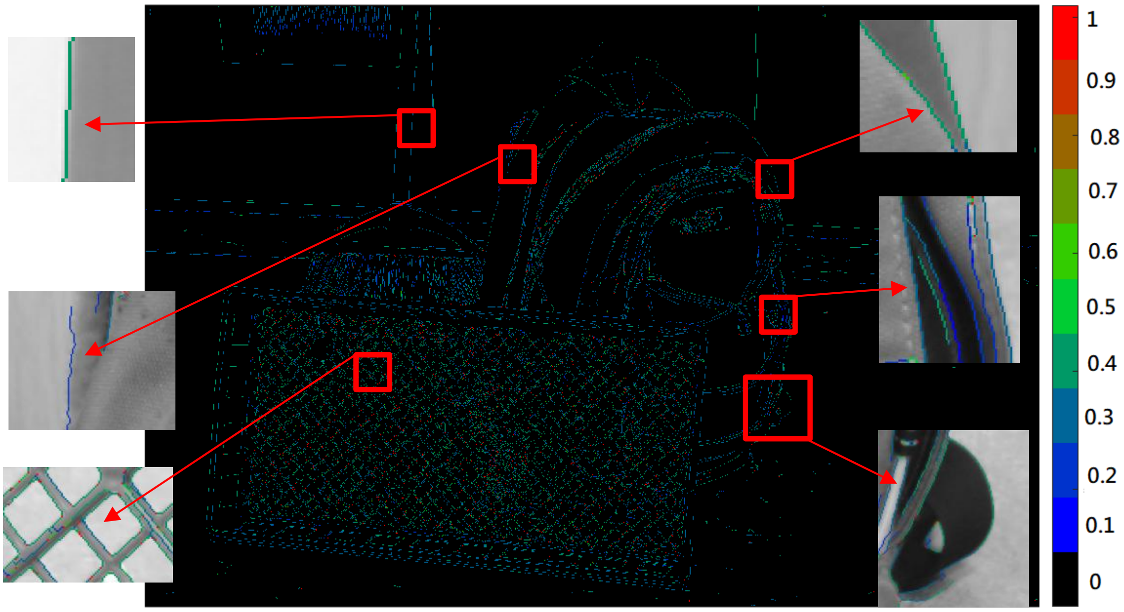


Figure 9. The indicator values on the detected edges (Backpack).

The average possibility distribution of indicator value in different deviation level is shown in Figure 10. The possibility is 10 experimental images average. In Figure 10, the bar represents the indicator's deviation possibility. For example, if the indicator is in the range 0.5~0.6, this edge will have about 90% possibility subpixel accuracy, 10% possibility accuracy more than one pixel, and 30% possibility accuracy smaller than 0.1 pixel in subpixel accuracy. The line chart represents the indicator percentage in the entire detected edges. It can see that the too big or too small indicator takes very small ratio in the entire detected edges. So maybe these too big or too small indicator not follows the rule, "The bigger indicator, the smaller deviation possibility" that we expect. They don't affect the entire quality evaluation because the ratio of them is too small, which can be ignored. Based on it, the too small or too big indicator can be denied in the future work, in order to avoid using unstable quality information.

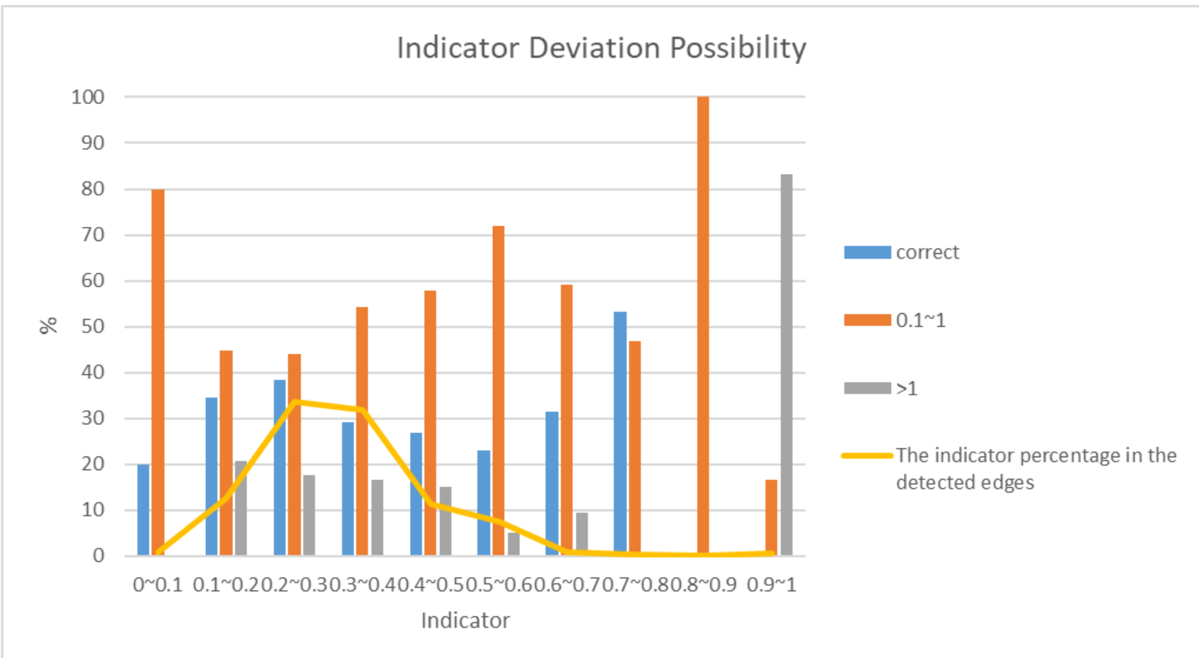


Figure 10. The average possibility distribution of indicator value in 3-kinds deviation level.

According to the Figure 10, we can expect the detected edge deviation and deviation possibility. With this information, this approach can give precise constraint to support dense stereo matching.

In the quality of matching subpixel disparity, we just take six obvious samples identified by human eyes. It is because this research wants to avoid automated matching error that makes quality unreliable. The matching samples are shown in Figure 11, and the matching quality is shown in Table 3.

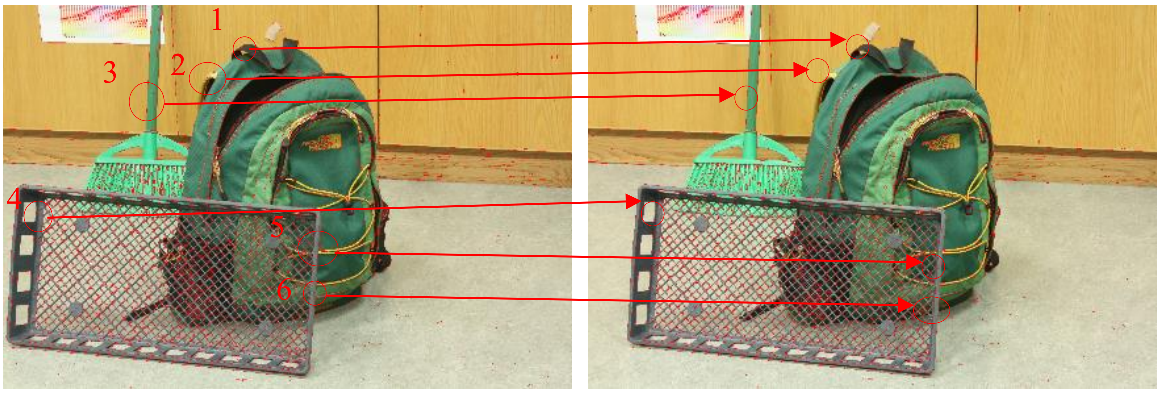


Figure 11. The sample of edge matching. (Backpack)

Table 3. The matching quality of samples.

| No | Disparity error (pixel) | Indicator (L/R) | | Thumbnail |
|---|---|---|---|---|
| 1 | -0.066 | 0.304 | 0.220 | |
| 2 | -1.1 | 0.148 | 0.161 | |
| 3 | 0.2583 | 0.267 | 0.230 | |
| 4 | 0.01 | 0.335 | 0.240 | |
| 5 | 0.305 | 0.242 | 0.183 | |
| 6 | 3.48 | 0.265 | 0.154 | |

In Table 3, we can see that the proposed method can support the subpixel accuracy depth to the depth discontinuities. The indicator also give some information of matching edge quality. If one of the indicator is too small, it tell users that these matching edges may be unreliable. When the following task uses these matching edges with indicator, the edges should be denied or cautiously employed based on the phenomenon that we find in Figure 10.

## 5. CONCLUTION AND FUTURE WORK

This research proposes the approach that support depth discontinuities with subpixel accuracy edge and priori quality indicator. The subpixel edges are based on the initial edge position computed by Edge Drawing, then refined to the subpixel accuracy by solving the image moment function. We weight the original moment function to ease the image noise. The moment weighting is quantified by the ideal gradient and difference of ideal gradient and observed gradient. The indicator is based on the image edge's S/N value to quantify edge priori quality. According to the result, the indicator can give some reliable quality information to help user choose better edge position and avoid using unreliable position. In the end, this research already have reliable subpixel edge information, the future work should be trying to have stable automated subpixel matching result.

## 6. REFERENCE

Agustín, T.P., Karl, K., Miguel, A.F., and Daniel, S.C., 2013. Accurate subpixel edge location based on partial area effect. Image and Vision Computing, 31(1), pp. 72-90.

Chang, Y. J., and Ho, Y. S., 2015. Disparity estimation using edge preserving method. TENCON 2015-2015 IEEE Region 10 Conference, pp.1-4.

Chen, J., Ian, D., Li, .S, Li, Z., Madden, M., Mills, J., Paparoditis, N., Rottensteiner, F., Sester, M., Toth, C., Trinder, J., and Heipke, C., 2016. Information from imagery: ISPRS scientific vision and research agenda. ISPRS Journal of Photogrammetry and Remote Sensing, 115, pp. 3-21.

Chuang, T. Y., Ting, H. W., and Jaw, J. J., 2016. Hybrid-Based Dense Stereo Matching. International Archives of the Photogrammetry, Remote Sensing and Spatial Information Sciences, Volume XLI-B3, pp.495-501.

ÇIĞLA, C., and Alatan, A.A., 2011. Efficient edge-preserving stereo matching. Computer Vision Workshops (ICCV Workshops) 2011 IEEE International Conference, pp.696-699.

Gu, J., Pan, Y., and Wang, H., 2015. Research on the improvement of image edge detection algorithm based on artificial neural network. Optik-International Journal for Light and Electron Optics, 126(21), pp. 2974-2978.

Gupta, S., Gupta, C., and Chakarvarti, S. K., 2013. Image Edge Detection: A Review. International Journal of Advanced Research in Computer Engineering & Technology (IJARCET), 1(2), pp. 2246-2251.

Hagara, M., and Kulla, P., 2011. Edge detection with sub-pixel accuracy based on approximation of edge with Erf function. Radioengineering, 20(2), 516-524.

Hermosilla, T., Bermejo, E., Balaguer, A., and Ruiz, L. A., 2008. Non-linear fourth-order image interpolation for subpixel edge detection and localization. Image and vision computing, 26(9):pp. 1240-1248.

Hwang, J. W., and Lee, H. S., 2004. Adaptive image interpolation based on local gradient features. IEEE Signal Processing Letters, 11(3), pp. 359-362.

Lee, H.C., 2016. Semi-Global Matching by Integrating Edge Feature Information, Thesis, National Taiwan University, Taipei, Taiwan. (in Chinese)

Lyvers, E. P., Mitchell, O. R., Akey, M. L., and Reeves, A. P., 1989. Subpixel measurements using a moment-based edge operator. IEEE Transactions on pattern analysis and machine intelligence, 11(12), pp.1293-1309.

Maini, R. and Aggarwal, H., 2009. Study and comparison of various image edge detection techniques. International journal of image processing (IJIP), 3(1), pp. 1-11.

Qu, Y.D., Cui, C.S., Chen, S.B., and Li, J.Q., 2005. A fast subpixel edge detection method using Sobel–Zernike moments operator. Image and Vision Computing, 23(1), pp.11-17.

Scharstein, D., Hirschmüller, H., Kitajima, Y., Krathwohl, G., Nešić, N., Wang, X., and Westling, P., 2014. High-resolution stereo datasets with subpixel-accurate ground truth. German Conference on Pattern Recognition, pp. 31-42.

Sun, X., Mei, X., Jiao, S., Zhou, M., Liu, Z., and Wang, H., 2014. Real-time local stereo via edge-aware disparity propagation. Pattern Recognition Letters, 49, pp. 201-206.

Tabatabai, A. J., and Mitchell, O. R., 1984. Edge location to subpixel values in digital imagery. IEEE transactions on pattern analysis and machine intelligence, (2), pp.188-201.

Topal, C., and Akinlar, C., 2012. Edge Drawing: A combined real-time edge and segment detector. Journal of Visual Communication and Image Representation, 23(6), pp. 862-872.

Wei, W., and Ngan, K. N., 2005. Disparity estimation with edge-based matching and interpolation. International Symposium on Intelligent Signal Processing and Communication Systems, pp. 153-156.